applied sciences

MDPI

Article

Acoustic Emission-Based Multi-Parameter Optimization of Remolding Conditions for Tectonic Coal: An Orthogonal Experimental Study

Congyu Zhong [1,3,†], Yutong Fu [2,*,†], Jingjing Liu [2,*], Jinting Xiong [2,3], Weilin Yuan [2] and Ruosi Zhao [2]

1 Institute of Experimental Testing, Guangzhou Marine Geological Survey, China Geological Survey, Guangzhou 510075, China; zhongcy@cumt.edu.cn
2 Sanya Institute of South China Sea Geology, Guangzhou Marine Geological Survey, China Geological Survey, Sanya 572024, China
3 School of Resources and Geosciences, China University of Mining and Technology, Xuzhou 221000, China
* Correspondence: fytxuzhidan@163.com (Y.F.); liujingjing@chd.edu.cn (J.L.); Tel.: +86-15162140889 (Y.F.); +86-18629018450 (J.L.)
† These authors contributed equally to this work.

Abstract

Tectonic coal, highly fragmented by geological stresses, cannot be sampled as intact specimens, making remolded (briquette) samples essential for mechanical testing. However, remolding conditions, particle grading, molding pressure, and moisture content, are typically selected empirically, lacking objective evaluation criteria. This study proposes an acoustic emission (AE)-based multi-parameter framework to optimize these conditions. Using an orthogonal design (three factors at three levels), we prepared remolded tectonic coal samples with varying gradings (1:1:1, 1:4:1, 1:8:1), pressures (15 MPa, 20 MPa, 25 MPa), and moisture contents (8%, 10%, 12%). Uniaxial compression tests were conducted, and five evaluation parameters were extracted: compressive strength, cumulative AE count, cumulative AE energy, energy conversion ratio k, and shear crack proportion r. Results show that AE parameters effectively reflect remolding quality in terms of signal activity, damage mode, and energy efficiency. Grading and pressure dominate cumulative AE metrics, while moisture content and pressure control k and r. Increasing medium-particle proportion or pressure enhances AE activity, k, and r; increasing moisture content suppresses them. The optimal remolding conditions for the studied coal are 1:8:1 grading, 25 MPa pressure, and 8% moisture content, with different condition priority sequences depending on optimization goals. This AE-based approach provides an objective, quantitative tool for tectonic coal remolding optimization, benefiting subsequent mechanical and permeability studies.

Keywords: tectonic coal; acoustic emission; remolding optimization; orthogonal experiment; energy conversion

Check for updates

Academic Editor: Andrea Carpinteri

Received: 4 June 2026
Revised: 6 July 2026
Accepted: 7 July 2026
Published: 14 July 2026

1. Introduction

Tectonic coal forms when primary coal undergoes brittle fragmentation, cataclasis, or ductile deformation under long-term tectonic stress [1,2]. Its reservoirs hold substantial coalbed methane (CBM), but mining frequently faces coal and gas outburst threats [3,4]. Over 90% of outburst disasters in major coal-producing regions—including Australia, North America, Europe, and Asia—occur in intensely deformed zones. In China, tectonic coal reserves are estimated at 457 billion tons, accounting for 23.5% of the total coal reserves [5]. Understanding tectonic coal's mechanical properties is therefore essential for improving CBM extraction and reducing outburst risk. However, due to severe structural destruction, tectonic coal typically exists in fragmented, granular, or powdered forms and exhibits much lower strength than intact coal, with ideal-plastic post-peak behavior and a negligible stress drop, and an elastic modulus and cohesion of only 15.5% and 26.5% of those of intact coal [6]. Consequently, obtaining high-quality intact samples is extremely difficult, and thus remolded (briquette) samples are widely used as substitutes to study their mechanical properties and failure mechanisms [7].

Extensive efforts have been devoted to preparing remolded tectonic coal samples with various experimental conditions. These studies have examined the effects of multiple factors, including particle size distribution, molding pressure, moisture content, binder type and dosage, and molding temperature, on the physical and mechanical properties of remolded coals. For example, Pang et al. investigated the influence of particle size on the mechanical properties of briquette samples and found that the original particle size distribution yielded the highest strength [8]. Ji et al. and Tian et al. highlighted the critical role of medium-sized particles in determining the structural integrity and strength of coal briquettes [9,10]. Xu et al. examined the effects of binder ratio on the mechanical and permeability characteristics of molded coal [11]. Skoczylas et al. explored the relationship between mechanical properties and outburst risk in coal briquettes prepared under varying pressures [12]. Meanwhile, recent advances have also been made in hot-pressed briquette technology: Xu et al. developed an optimization method combining the Markov distance measurement and the golden section method, and reported that the optimal briquette prepared under 80 MPa molding pressure exhibited density, uniaxial compressive strength and initial permeability extremely close to those of raw coal [13]. These investigations have established the feasibility of using remolded tectonic coal as an analog for studying its mechanical behavior and have identified several key factors that influence remolding quality [14–16].

Despite these contributions, most existing studies have selected remolding conditions primarily based on empirical approaches or on the reproduction of conditions reported in the previous literature [17,18]. In other words, the determination of particle grading, molding pressure, and moisture content has largely followed trial-and-error strategies, lacking objective and quantitative evaluation criteria to justify why a particular combination of conditions should be considered optimal [19,20]. As a result, the influence of these factors on the internal damage process, energy dissipation mechanisms, and fracture modes of remolded tectonic coal remains inadequately understood [21–23]. The lack of such systematic optimization not only limits the consistency and repeatability of experimental results across different studies, but also hinders the ability to tailor remolding conditions to specific research objectives, such as achieving mechanical property similarity, matching acoustic emission characteristics, or controlling damage modes. To address this gap, a systematic, evaluation parameter-driven optimization framework is needed to guide the selection of remolding conditions in a more rational and objective manner.

Acoustic emission (AE) technology has emerged as a powerful tool for monitoring the deformation and failure processes of coal and rock materials in a non-contact manner. When a coal sample undergoes deformation and fracture under loading, it releases elastic waves that can be captured by AE sensors and analyzed to characterize the initiation, propagation, and coalescence of microcracks. Recent research has demonstrated that AE parameters can effectively capture the entire process of damage evolution in coal samples. Shao et al. conducted uniaxial compression AE experiments on coal–rock combinations containing tectonic coal and analyzed the effects of coal thickness on AE count and event characteristics [22,24]. Wang et al. investigated the AE characteristics and energy evolution of water-bearing coal under uniaxial compression, revealing that increasing moisture content leads to a gradual decline in compressive strength and energy dissipation rate, and that moisture shifts the failure mode from oblique failure to axial splitting while decreasing the proportion of shear cracks [25]. Zhang et al. investigated the failure characteristics of coal samples with different bedding orientations using AE technology under uniaxial compression, analyzing the relationships among stress, strain, and AE parameters [26]. Xu et al. combined SEM, X-ray micro-CT, and AE monitoring to investigate damage evolution and failure precursors in coal under monotonic and cyclic loading, identifying an AE quiet period before peak stress as a predictor of failure [27]. Moreover, the RA (rise time/amplitude) and AF (average frequency) parameters have been widely applied to qualitatively identify crack types during coal failure: AE events with low RA and high AF are associated with tensile cracking, whereas those with high RA and low AF indicate shear-dominated failure [28]. By analyzing the RA-AF distribution, the proportion of shear cracks in the overall failure process can be quantified, providing an effective means for evaluating the damage mode of remolded samples.

Given that remolded tectonic coal also releases elastic waves during its deformation and failure process, AE technology can be readily applied to assess remolding quality from multiple perspectives [29,30]. Compared with traditional evaluation methods that rely solely on mechanical strength or density measurements, AE-based parameters offer the distinct advantage of providing continuous, real-time information on the entire damage process, including crack initiation, propagation, and coalescence stages [31,32]. This enables a more comprehensive assessment of how different remolding conditions affect the internal structure and failure behavior of the remolded samples. Furthermore, by extracting evaluation parameters related to signal intensity, energy conversion efficiency, and damage mode, AE technology can serve as a powerful tool for objectively comparing and optimizing remolding conditions [33–35]. However, despite its potential, few studies have systematically employed AE parameters to guide the optimization of tectonic coal remolding [36].

In light of the above, this study aims to establish an AE-based multi-parameter optimization framework for determining the optimal remolding conditions of tectonic coal. Specifically, remolded tectonic coal samples were prepared under orthogonal combinations of three factors (particle grading, molding pressure, and moisture content) at three levels each. Uniaxial compression tests were conducted on these samples with simultaneous AE monitoring to extract five evaluation parameters: uniaxial compressive strength, cumulative AE count, cumulative AE energy, energy conversion ratio k (AE energy density/input energy density), and shear crack proportion r (derived from RA–AF analysis). Through range analysis and variance analysis of the orthogonal experimental results, the sensitivity of each evaluation parameter to different remolding conditions was determined, the underlying mechanisms influencing AE activity, energy conversion and damage mode were interpreted, and a set of goal-oriented optimization strategies was proposed. The findings provide a quantitative, objective basis for the preparation of reliable remolded tectonic coal specimens, which is of practical significance for subsequent studies on the mechanical behavior, permeability evolution, and gas extraction safety of tectonic coal reservoirs.

2. Materials and Methods

2.1. Source of Tectonic Coal

The tectonic coal used in this study was collected from the 1216(1) working face of the 11-2 coal seam in the Zhangji coal mine, Huainan coalfield, China. The sampling location is structurally complex, with multiple tectonic regimes controlling the deposit. The in situ tectonic coal appears in fragmented, granular, and powdered forms (Figure 1). After recovery, the raw coal was sieved and stored as the base material for remolding.

https://doi.org/10.3390/app16147057

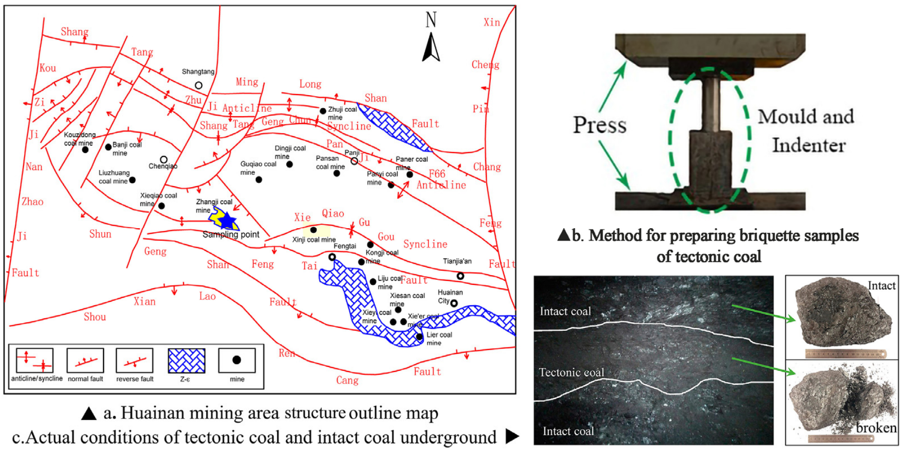

Figure 1. Tectonic outline of the mining area, in situ tectonic coal, and mold for briquetting [37].

2.2. Sample Preparation and Testing Procedure

2.2.1. Remolding Condition and Preparation

Three remolding factors were investigated at three levels each, following an orthogonal experimental design (L_9):

Molding pressure: 15 MPa, 20 MPa, 25 MPa. The selection was based on the in situ stress of the sampling area (13–15 MPa) extended appropriately to explore the optimization range. This upper limit was selected based on preliminary compaction tests, which showed that beyond 25 MPa, the density and mechanical properties of the briquette samples reach a plateau with negligible improvement, while the risk of sample damage increases. This range also covers the typical pressures reported in previous studies on remolded coal specimens, ensuring comparability.

Particle grading: Three size fractions were obtained by sieving: coarse (5 mm $< d <$ 20 mm), medium (0.2 mm $< d \leq$ 5 mm), and fine ($d \leq$ 0.2 mm). Based on the recognized importance of medium particles, three mass ratios (coarse:medium:fine) were designed: 1:1:1, 1:4:1, and 1:8:1.

Moisture content: 8%, 10%, and 12% (by weight). Distilled water was added and mixed uniformly.

For each orthogonal combination (Table 1), the weighed coal particles were homogenized in a mixer, and then placed into a cylindrical steel mold with an inner diameter of 50 mm. The mixture was statically pressed using a universal testing machine (EAST, Jinhua, China) at a loading rate of 1 mm/min until the target pressure was reached, held for 5 min, and then unloaded. The obtained cylindrical samples (height $\approx$ 100 mm) were polished at both ends to ensure parallelism. At least three replicate samples were prepared for each condition.

Table 1. Tectonic coal orthogonal sample-making schemes.

Conditions	Level		Number	Content
Molding Pressure	I	15 MPa	Ot-1	1:1:1; 15 MPa; 8%
	II	20 MPa	Ot-2	1:1:1; 20 MPs; 10%
	III	25 MPa	Ot-3	1:1:1; 25 MPa; 12%
Grading	I	1:1:1	Ot-4	1:4:1; 15 MPa; 10%
	II	1:4:1	Ot-5	1:4:1; 20 MPa; 12%
	III	1:8:1	Ot-6	1:4:1; 25 MPa; 8%
Moisture Content	I	8%	Ot-7	1:8:1; 15 MPa; 12%
	II	10%	Ot-8	1:8:1; 20 MPa; 8%
	III	12%	Ot-9	1:8:1; 25 MPa; 10%

2.2.2. Uniaxial Compression Test with AE Monitoring

Uniaxial compression tests were performed using the same universal testing machine under displacement control at a rate of 0.5 mm/min. The axial load and displacement were recorded automatically. During loading, acoustic emission signals were acquired using a DS5-16B AE signal analyzer (Beijing Soft Island, Beijing, China). A resonant piezoelectric sensor (frequency range 100–500 kHz, resonant frequency 150 kHz) was attached to the sample surface using vacuum grease as a couplant. The preamplifier gain was set to 40 dB, the threshold to 45 dB, and the sampling rate to 1 MHz. A 40 dB low-pass filter was applied to eliminate background noise, as shown in Figure 2.

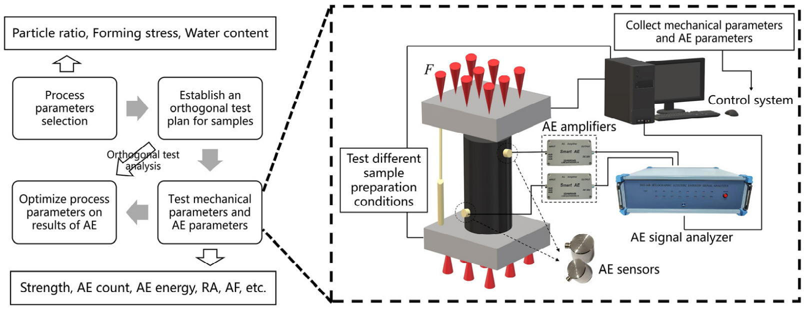

Figure 2. Experimental design and test program.

2.3. Evaluation Parameters

2.3.1. Cumulative AE Count and Cumulative AE Energy

When the release of an elastic wave exceeds the detection threshold of the instrumentation, it is recognized as one acoustic emission event, corresponding to a hit. The duration of this process defines the event duration, while the period from onset to the maximum amplitude is referred to as the rise time. Within a single AE event, all peaks exceeding the threshold are recorded as counts. The integral profile of the waveform can be used to represent the energy required to generate the AE event [38]. The ringing count and energy of AE signals reflect the intensity of microcracking within the sample. Cumulative AE count and cumulative AE energy were extracted as basic evaluation parameters.

2.3.2. *r* Value: Shear Crack Proportion

The RA value (rise time/amplitude) and AF value (ring count/duration) serve as key indicators for identifying crack types: tensile cracking is typically associated with a low RA and high AF, whereas shear cracking corresponds to a high RA and low AF [17,18]. The threshold is defined as Equation (1).

$$\mathrm{C} = \frac{\mathrm{AF}}{\mathrm{RA}} \tag{1}$$

The r value is the proportion of AE events with AF/RA < 1, representing the shear crack proportion, shown in Equation (2).

$$r = \frac{N_c}{N_0} \times 100\% \tag{2}$$

where N_C is the number of events with AF/RA < 1 and N_0 is the total number of AE events.

2.3.3. *k* Value: Energy Conversion Ratio

The AE energy density E_{d1} ($\mathrm{J \cdot mm^{-3}}$) is calculated by Equation (3).

$$E_{d1} = \frac{E_1}{V} = \frac{1}{V} \int_{t_0}^{t} \frac{U^2}{R} dt \tag{3}$$

where U is the transducer voltage (V), R the internal resistance (Ω), and V the sample volume (mm^3). The input energy density E_{d2} ($J{\cdot}mm^{-3}$) from the press work is calculated by Equation (4), which can be obtain by work curve of press.

$$E_{d2} = \frac{E_2}{V} = \frac{1}{V}\int_0^{s_m} F ds \tag{4}$$

with F as the axial load (kN) and s_m the axial displacement (mm). The k value is shown as Equation (5).

$$k = E_{d1}/E_{d2} \tag{5}$$

It represents the proportion of input energy converted into detectable AE energy, reflecting the brittleness and crack propagation efficiency of the remolded sample.

3. Results

3.1. Mechanical Parameters and Basic AE Parameters

The uniaxial compression test results are summarized in Table 2. These wide ranges indicate that the remolding conditions significantly affect the mechanical behavior of the tectonic coal samples. Figure 3 superimposes the ringing count signal, AE energy signal, and stress–strain curve for selected samples (Ot-1, Ot-2, Ot-7) alongside an intact coal sample. The stress–strain curves of remolded tectonic coals exhibit four typical stages: compression (pore collapse), elastic deformation, plastic yielding, and post-peak failure.

Table 2. Uniaxial compression test results.

No.	Ot-1	Ot-2	Ot-3	Ot-4	Ot-5	Ot-6	Ot-7	Ot-8	Ot-9
σ_m/MPa	0.90	1.15	1.23	0.67	0.91	0.62	0.78	1.11	1.04
E/MPa	89.42	86.37	93.61	50.04	79.83	49.18	76.69	122.64	96.55
M/MPa	−87.22	−106.91	−160.12	−45.76	−67.32	−177.61	−82.13	−116.33	−110.71

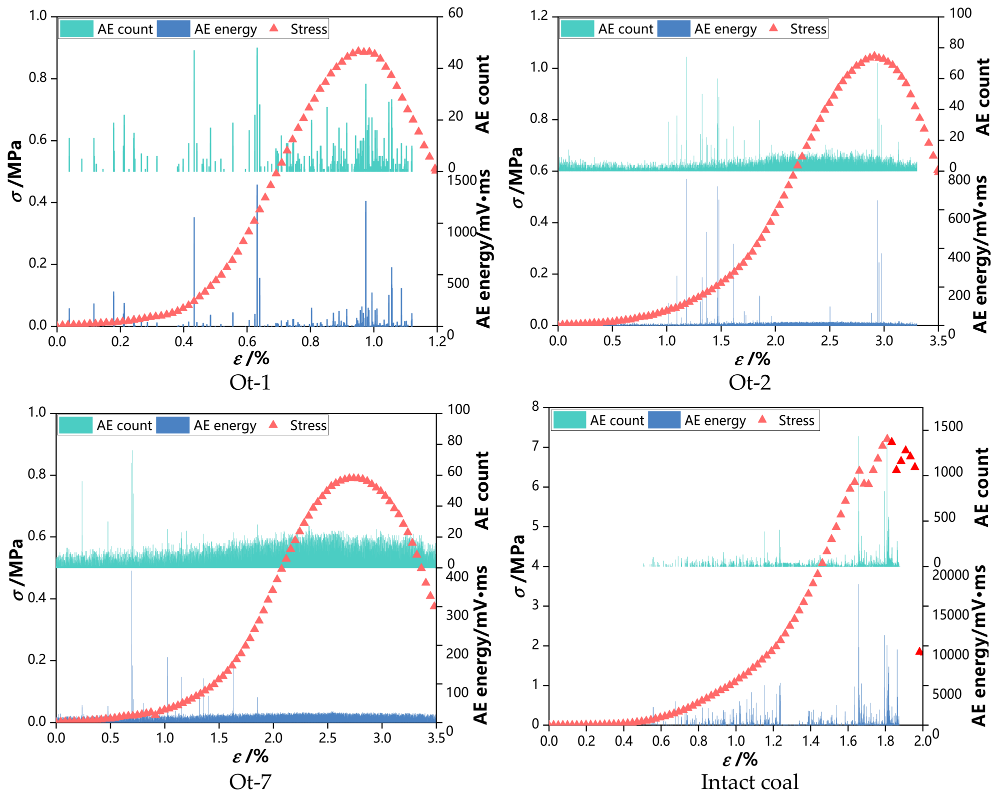

Figure 3. Partial acoustic emission test results and intact coal test results.

The AE signals correspond well with these stages. Specifically,

- In the compression and plastic yielding stages, both the ringing count and AE energy increase, coinciding with changes in the slope of the stress–strain curve.
- Immediately before the post-peak failure stage, a sudden surge in both ringing count and AE energy occurs.
- Throughout the entire loading process, AE signals remain continuously active, indicating progressive damage accumulation.

3.2. AF-RA Analysis and r Value

The AF (average frequency) and RA (rise time/amplitude) values for representative remolded samples and an intact coal sample are shown in Figure 4. The corresponding r values (proportion of shear cracks) are listed in Table 3.

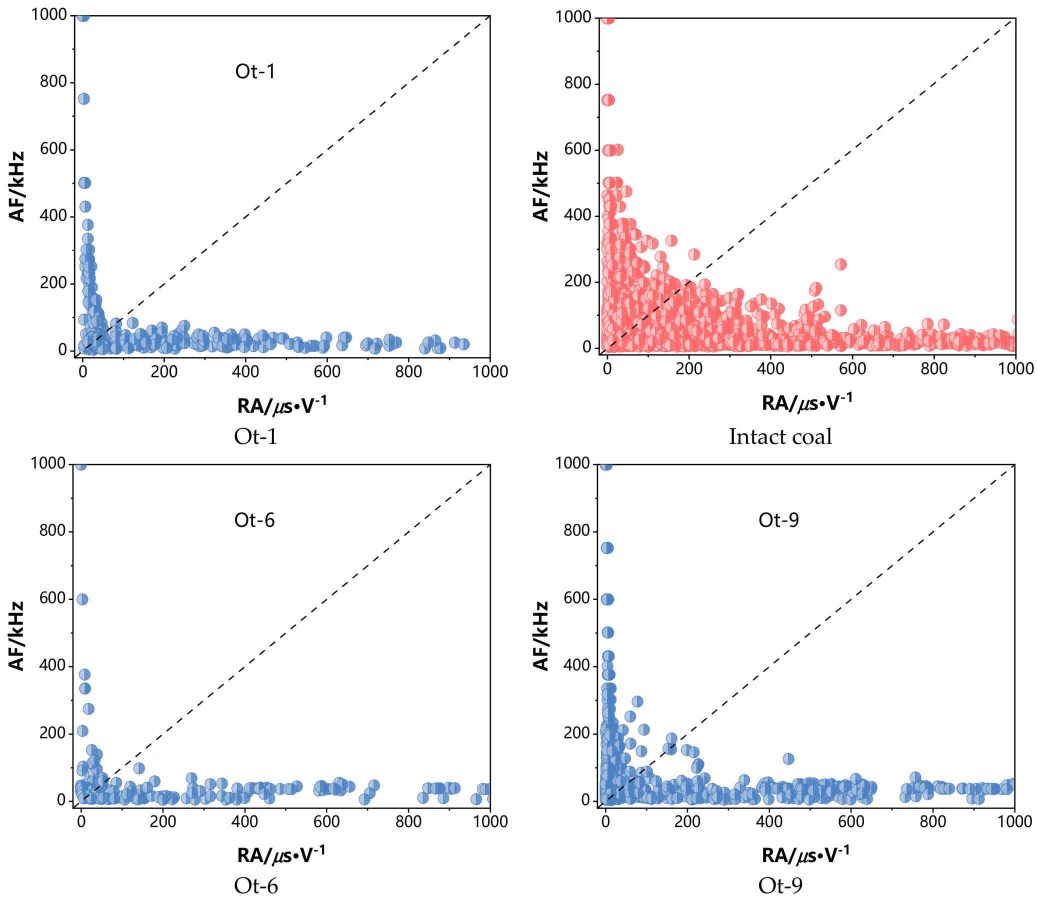

Figure 4. Partial AF-RA and intact coal AF-RA value results.

Table 3. r values.

No.	Ot-1	Ot-2	Ot-3	Ot-4	Ot-5	Ot-6	Ot-7	Ot-8	Ot-9	RC
r/%	61.34	28.7	68	43.24	45.7	86.2	40.22	79.22	73.4	65.1

As shown in Figure 4, for all remolded samples, the data points are relatively sparse compared with intact coal, and most points fall into the region associated with shear-dominant cracking (high RA, low AF). This indicates that the failure of remolded tectonic coal is a tension–shear composite mode, with shear cracking playing a dominant role. The intact coal exhibits a dense cluster of points also concentrated in the shear region, with an r value of 65.1%. Among the remolded samples, the r value varies considerably from 28.7%

(Ot-2) to 86.2% (Ot-6). The wide variation suggests that remolding conditions strongly influence the failure mode. Higher *r* values (closer to intact coal) are generally associated with better interparticle contact and higher compaction.

The threshold $r = 1$ was selected based on the natural clustering of AE events in the data space observed in our preliminary analysis, where tensile-dominated events generally exhibit AF/RA > 1 and shear-dominated events exhibit AF/RA < 1. This fixed criterion ensures consistent and objective comparison across all experimental groups.

3.3. Energy Density and k Value

Figure 5 presents the AE energy release density E_{d1}, the input energy density E_{d2}, and the energy conversion ratio *k* for all remolded samples and intact coal. The intact coal shows an E_{d2} of approximately 0.25 J·mm^{-3}, whereas most remolded samples have much lower values (typically <0.10 J·mm^{-3}), indicating that less energy is required to fracture the remolded material.

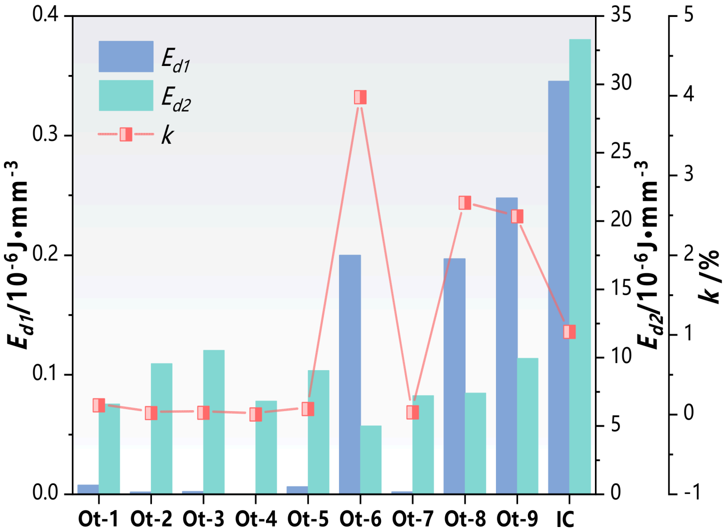

Figure 5. Energy density value and *k* value test result.

The *k* value, which represents the proportion of input energy converted into detectable AE energy, ranges from nearly 0% (Ot-1, Ot-2, Ot-3, Ot-4, Ot-5, Ot-7) to 3.98% (Ot-6). Intact coal has a *k* value of 0.91%. The large variation in k suggests that the efficiency of elastic wave generation, hence the brittleness of the coal material, is highly sensitive to remolding conditions. Samples with higher *k* (e.g., Ot-6, Ot-8, Ot-9) exhibit more brittle, AE-active failure, which is desirable for mimicking intact coal behavior.

4. Discussion

4.1. Sensitivity of Evaluation Parameters to Remolding Conditions

The range analysis and variance analysis of the orthogonal experimental results (Table 4) reveal distinct sensitivity patterns among the five evaluation parameters. Particle grading and molding pressure have stronger effects on uniaxial compressive strength, cumulative AE count, and cumulative AE energy than moisture content does. In contrast, moisture content and molding pressure dominate the variations in the energy conversion ratio k and the shear crack proportion *r*. This differential sensitivity arises from the distinct physical roles of the three factors in the briquetting process.

Table 4. Results of evaluation parameters.

Number	σ_m/MPa	Cumulative AE Counts	Cumulative AE Energy/mV·ms	k/%	r/%
Ot-1	0.90	19,021	21,329.11	0.12	61.34
Ot-2	1.15	23,845	46,579.77	0.02	28.70
Ot-3	1.23	123,968	131,189.05	0.02	68
Ot-4	0.67	61,842	70,893.44	0	43.24
Ot-5	0.91	117,583	227,975.8	0.07	45.70
Ot-6	0.62	165,624	272,487.7	3.98	86.2
Ot-7	0.78	42,926	72,139.6	0.03	40.22
Ot-8	1.11	224,456	366,356.2	2.66	79.22
Ot-9	1.04	230,315	317,388	2.49	73.4

Particle grading determines the initial packing density and the connectivity of the particle contact network. A higher proportion of medium particles (e.g., the 1:8:1 grading) fills the interstices between coarse particles, creating a more continuous and interlocked skeleton. Under uniaxial loading, this skeleton transmits stress more efficiently, leading to widespread microcracking and thus higher AE counts and cumulative AE energy (Table 4: Ot-9 vs. Ot-1). Conversely, a uniform grading (e.g., 1:1:1) leaves larger voids that collapse under load, producing fewer but larger fracture events—hence lower cumulative AE metrics.

Molding pressure directly controls the degree of compaction. Higher pressure (25 MPa) forces particles into closer contact, increases frictional resistance and mechanical interlocking, and reduces porosity. During subsequent loading, the densified sample stores more elastic energy before failure and releases it more abruptly, generating stronger AE signals. Low pressure (15 MPa) yields a loose structure that undergoes gradual, ductile deformation with less intense AE activity.

Moisture content plays a dual role depending on its level. At low content (8%), water acts as a binder through capillary forces and surface tension, enhancing cohesion without fully saturating the pore space. At higher contents (10–12%), excess water lubricates particle contacts, reduces friction, and promotes particle rearrangement without brittle fracture, thereby suppressing AE activity. This explains why higher moisture content reduces cumulative AE counts, k, and r (Table 4: Ot-6 vs. Ot-7).

4.2. Mechanisms Controlling the Energy Conversion Ratio k

The k value reflects the efficiency with which input mechanical energy is converted into detectable AE energy. A higher k indicates that a larger proportion of the input energy is dissipated via brittle microcracking rather than through plastic deformation or frictional heat.

Why do increasing medium-particle proportion and molding pressure increase k? A well-graded, highly compacted sample forms a rigid load-bearing framework. Under axial loading, stress concentrates at particle contacts, triggering local tensile and shear failures that generate elastic waves efficiently. The limited porosity restricts particle rearrangement, so most input energy is consumed in crack propagation—yielding a high k. In contrast, a loose or poorly graded sample undergoes substantial pore collapse and particle sliding, dissipating energy through friction and plastic flow, which produces weaker AE and a lower k.

Why does increasing moisture content decrease k? Water reduces the effective stress at particle contacts by increasing pore pressure and lowers the friction coefficient. This shifts the failure mode from brittle fracturing to ductile yielding. In water-rich samples, particles slide past each other rather than snapping, so the stored elastic energy is dissipated as heat and viscous flow rather than as high-frequency AE. Consequently, k drops sharply from 3.98% (Ot-6, 8% moisture) to 0.03% (Ot-7, 12% moisture).

4.3. Mechanisms Controlling the Shear Crack Proportion r

The *r* value represents the proportion of shear-dominant AE events. A higher r indicates that shear failure (Mode II/III) dominates over tensile failure (Mode I), which is typical of compact, confined materials.

Effect of grading and pressure: Dense packing and high pressure increase interparticle friction and normal stress at contacts, promoting shear failure. This is consistent with Ot-6 (1:8:1, 25 MPa) having the highest r (86.2%) and Ot-2 (1:1:1, 20 MPa) the lowest (28.7%).

Effect of moisture content: Water lubricates contacts, reducing the shear resistance. Under lubrication, tensile cracks—which require lower shear stress—become relatively more favorable, decreasing the proportion of shear events. This explains why Ot-7 (12% moisture) has a lower *r* (40.22%) than Ot-6 (8% moisture, 86.2%), even under otherwise similar conditions.

4.4. Implications for Optimizing Remolding Conditions

The mechanistic understanding above enables a goal-oriented optimization strategy.

(1) For maximizing mechanical strength: Prioritize grading to achieve a dense skeleton (e.g., 1:8:1), then increase molding pressure, and finally reduce moisture content. Strength is most sensitive to grading (Figure 6), because a stable grain arrangement is the primary load-bearing structure.

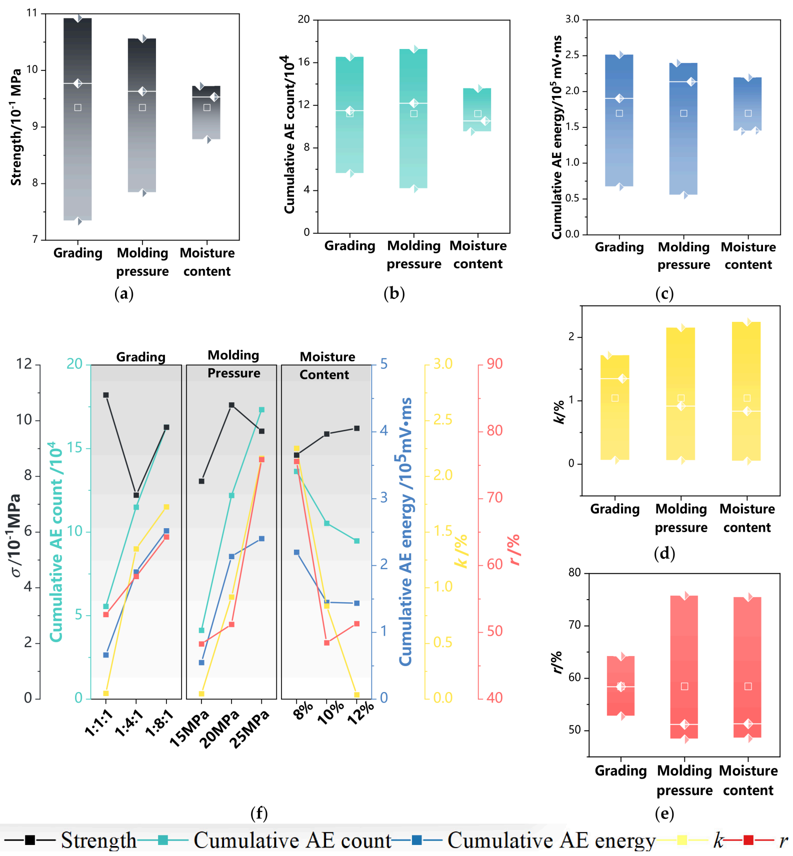

Figure 6. Influence scope and variation trend of evolution parameters. (**a**) Schematic diagram of strength analysis of variance. (**b**) Schematic diagram of cumulative AE count analysis of variance. (**c**) Schematic diagram of cumulative AE energy analysis of variance. (**d**) Schematic diagram of *k* value analysis of variance. (**e**) Schematic diagram of *r* value analysis of variance. (**f**) Schematic diagram of variation trend of evolution parameters.

(2) For achieving AE signal similarity to intact coal: Intact coal typically exhibits intense AE activity and shear-dominant failure. Therefore, increase molding pressure first to enhance interlocking and brittle response, then increase the medium-particle proportion, and finally reduce moisture content to avoid lubrication.
(3) For matching energy conversion (k) and damage mode (r): These are most sensitive to moisture content (Figure 6). Hence, reduce moisture content first to minimize ductile behavior, then increase molding pressure to raise k and r, and finally adjust grading.

Based on a comprehensive consideration of all evaluation parameters, the optimal remolding conditions for the Zhangji mine tectonic coal are determined as: coarse:medium:fine grading = 1:8:1, molding pressure = 25 MPa, and moisture content = 8%. Under these conditions, the remolded sample exhibits the best overall similarity to intact coal in terms of mechanical strength, AE activity, energy conversion efficiency, and shear crack proportion.

5. Conclusions

This study demonstrates that acoustic emission (AE) parameters can serve as objective and quantitative indicators for optimizing the remolding conditions of tectonic coal. Based on uniaxial compression tests with AE monitoring on remolded samples prepared under orthogonal combinations of particle grading, molding pressure, and moisture content, the following conclusions are drawn.

1. AE-based evaluation parameters effectively discriminate remolding quality. Cumulative AE count, cumulative AE energy, the energy conversion ratio k, and the shear crack proportion r reflect the signal activity, energy dissipation, and damage mode of remolded tectonic coal, providing a reliable basis for optimization.
2. Sensitivity of evaluation parameters to remolding conditions differs. Particle grading and molding pressure dominate cumulative AE count and energy, whereas moisture content and molding pressure primarily control k and r. This differential sensitivity guides the selection of adjustment priorities for different optimization goals.
3. Increasing the medium-particle proportion or molding pressure enhances AE activity, k, and r; conversely, increasing moisture content suppresses these parameters. Strength exhibits a more complex trend: it first decreases and then increases with increasing medium-particle proportion, and first increases and then decreases with increasing molding pressure.
4. The optimal remolding conditions for the studied tectonic coal are a coarse:medium:fine grading of 1:8:1, a molding pressure of 25 MPa, and a moisture content of 8%. For different optimization goals, the priority sequence of condition adjustments varies: for strength, prioritize grading; for AE signal similarity to intact coal, prioritize pressure; for energy conversion and damage mode, prioritize reducing moisture content.

This AE-based multi-parameter optimization framework provides a practical and objective tool for preparing reliable remolded tectonic coal specimens, which is essential for subsequent studies on the mechanical behavior, permeability evolution, and gas extraction safety of tectonic coal reservoirs.

Author Contributions: Conceptualization, C.Z. and Y.F.; methodology, C.Z.; validation, J.X., W.Y. and R.Z.; formal analysis, Y.F.; investigation, J.X. and W.Y.; writing—original draft preparation, C.Z.; writing—review and editing, C.Z. and Y.F.; visualization, C.Z.; supervision, J.L.; project administration, J.L.; funding acquisition, Y.F. and J.L. All authors have read and agreed to the published version of the manuscript.

Funding: This research was funded by the Director General's Scientific Research Fund of Guangzhou Marine Geological Survey, grant numbers 2023GMGSJZJJ00029 and 2025GMGSQN17.

Institutional Review Board Statement: Not applicable.

Informed Consent Statement: Not applicable.

Data Availability Statement: The authors of the paper declare that all data comes from original experiments.

Acknowledgments: The authors are grateful for the support of the laboratory of School Resources and Geosciences and the laboratory of Guangzhou Marine Geological Survey.

Conflicts of Interest: The authors declare no conflicts of interest.

References

1. Tu, Q.; Cheng, Y.; Xue, S.; Ren, T.; Cheng, X. Analysis of the Coal and Gas Outburst Mechanism from the Perspective of Tectonic Movement. *Geofluids* **2021**, *2021*, 9988420. [CrossRef]
2. Li, L.; Liu, D.; Cai, Y.; Wang, Y.; Jia, Q. Coal Structure and Its Implications for Coalbed Methane Exploitation: A Review. *Energy Fuels* **2021**, *35*, 86–110. [CrossRef]
3. Wang, D.; Cheng, Y.; Yuan, L.; Wang, L.; Zhou, H. Experimental Study of Multiple Physical Properties of Tectonic Coal near a Minor Fault: Implications for Coal and Gas Outburst. *Energy Fuels* **2023**, *37*, 5878–5894. [CrossRef]
4. Zhu, M.; Jing, T.; Yuan, H.; Zhang, J. Effect of Tectonic Deformation on the Pore System and Methane Adsorption of Anthracite Coal. *ACS Omega* **2024**, *9*, 34250–34258. [CrossRef] [PubMed]
5. Cheng, Y.; Pan, Z. Reservoir Properties of Chinese Tectonic Coal: A Review. *Fuel* **2020**, *260*, 116350. [CrossRef]
6. Zhang, F.; Niu, C.; Han, Y. Evolution of the Strength Characteristics of Briquette and Raw Coal Containing Fluid. *Sci. Rep.* **2023**, *13*, 593. [CrossRef] [PubMed]
7. Meng, H.; Wu, L.; Yang, Y.; Wang, F.; Peng, L.; Li, L. Evolution of Mechanical Properties and Acoustic Emission Characteristics in Uniaxial Compression: Raw Coal Simulation Using Briquette Coal Samples with Different Binders. *ACS Omega* **2021**, *6*, 5518–5531. [CrossRef] [PubMed]
8. Pang, L.; Yang, Y.; Wu, L.; Wang, F.; Meng, H. Effect of Particle Sizes on the Physical and Mechanical Properties of Briquettes. *Energies* **2019**, *12*, 3618. [CrossRef]
9. Ji, D.; Wang, Z.; Zhang, L.; Ma, Y. The Examination Study of the Size-Composition of the Fine-Coal Briquetting. *J. China Coal Soc.* **2005**, *1*, 100–103. [CrossRef]
10. Tian, B.; Xu, D.; Yang, F.; Pang, Y.; Xu, R.; Lin, X.; Wang, Y. Briquetting Pressure and Fine Coal Particle Distribution Affected to Performances of Cool Pressed Briquette. *Coal Sci. Technol.* **2013**, *41*, 125–128.
11. Xu, J.; Ye, G.; Li, B.; Cao, J.; Zhang, M. Experimental Study on Mechanical and Permeability Characteristics of Briquette Coal under Different Binder Ratios. *Rock Soil Mech.* **2015**, *36*, 104–110. [CrossRef]
12. Skoczylas, N.; Dutka, B.; Sobczyk, J. Mechanical and Gaseous Properties of Coal Briquettes in Terms of Outburst Risk. *Fuel* **2014**, *134*, 45–52. [CrossRef]
13. Xu, J.; Jia, L.; Gan, Q.; Peng, S.; Yan, F.; Wang, X.; Dai, S.; Jiao, F.; Li, Q.; Chen, Y. Experimental Method for Optimization the Molding Conditions of Hot-pressed Briquette. *J. China Coal Soc.* **2024**, *49*, 739–752. [CrossRef]
14. Lai, X.; Zhang, S.; Cui, F.; Wang, Z.; Xu, H.; Fang, X. Energy Release Law during the Damage Evolution of Water-Bearing Coal and Rock and Pick-up of AE Signals of Key Pregnancy Disasters. *Chin. J. Rock Mech. Eng.* **2020**, *39*, 433–444.
15. Burud, N.B.; Kishen, J.M.C. Response Based Damage Assessment Using Acoustic Emission Energy for Plain Concrete. *Constr. Build. Mater.* **2021**, *269*, 121241. [CrossRef]
16. He, M.; Zhao, F.; Du, S.; Zheng, M. Rockburst Characteristics Based on Experimental Tests under Different Unloading Rates. *Rock Soil Mech.* **2014**, *35*, 2737–2747.
17. Aggelis, D.G. Classification of Cracking Mode in Concrete by Acoustic Emission Parameters. *Mech. Res. Commun.* **2011**, *38*, 153–157. [CrossRef]
18. Farhidzadeh, A.; Salamone, S.; Singla, P. A Probabilistic Approach for Damage Identification and Crack Mode Classification in Reinforced Concrete Structures. *J. Intell. Mater. Syst. Struct.* **2013**, *24*, 1722–1735. [CrossRef]
19. Cuccurullo, A.; Gallipoli, D.; Bruno, A.W.; Augarde, C.; Hughes, P.; La Borderie, C. A Comparative Study of the Effects of Particle Grading and Compaction Effort on the Strength and Stiffness of Earth Building Materials at Different Humidity Levels. *Constr. Build. Mater.* **2021**, *306*, 124770. [CrossRef]
20. Arif, M.; Awan, F.U.R.; Zhang, H.; Hosseini, M. Coal Wettability: A Holistic Overview of the Data Sets, Influencing Factors, and Knowledge Gaps. *Energy Fuels* **2024**, *38*, 15069–15084. [CrossRef]
21. Tan, Y.; Cheng, H.; He, M.; Guo, W.; Bai, E.; Li, H.; Guo, W.; Wang, Y.; Zhang, S.; Chang, B.; et al. Characterization of Acoustic Emission Parameters and Identification of Staged Fracture Propagation in Solidified Body-Coal Combination Based on Experimental and Machine Learning Approaches. *Sci. Rep.* **2026**, *16*, 8314. [CrossRef] [PubMed]

22. Wang, Y.; Deng, H.; Deng, Y.; Chen, K.; He, J. Study on Crack Dynamic Evolution and Damage-Fracture Mechanism of Rock with Pre-Existing Cracks Based on Acoustic Emission Location. *J. Pet. Sci. Eng.* **2021**, *201*, 108420. [CrossRef]
23. Wang, K.; Jiang, Y.; Xu, C. Mechanical Properties and Statistical Damage Model of Coal with Different Moisture Contents Under Uniaxial Compression. *Chin. J. Rock Mech. Eng.* **2018**, *37*, 1070–1079. [CrossRef]
24. Shao, Q.; Li, Q.; Zhao, P.; Ren, X.; Wang, X.; Tian, Y.; Li, S. Experimental Study on Acoustic Emission Characteristics of Loading Rupture of Tec-Tonic Coal Assembly. *J. Xi'an Univ. Sci. Technol.* **2024**, *44*, 279–288. [CrossRef]
25. Wang, X.; Wang, J.; Liu, X.; Liu, Y.; Chang, X.; Wu, J.; Zhou, X.; Labuz, J.F. Acoustic and Current from Fracturing of Loaded Coal at Various Water Saturations. *Nat. Resour. Res.* **2025**, *34*, 2797–2821. [CrossRef]
26. Zhang, C.; Ji, H.; Zhang, Y.; Fu, Z.; Song, Y.; Tian, Z.; Liu, H. Characteristics and differential analysis of energy evolutin of deep tectonic coal during fracturing processes. *J. Min. Strat. Control Eng.* **2025**, *7*, 063011–063020. [CrossRef]
27. Lu, H.; Xia, C.; Xu, C.; Wang, C.; Zhao, H.; Maruvanchery, V.; Li, G. Precursory Characteristics of Coal-Rock Failure Using Acoustic Emission and Computed Tomography under Uniaxial Monotonic and Cyclic Compression. *Measurement* **2025**, *247*, 116844. [CrossRef]
28. Ma, S.; Zhou, Y.; Ma, D. Research on Acoustic Emission Precursor Characteristics of Coal Sample Unloading Failure Based on Discrete Wavelet Analysis. *Sci. Rep.* **2024**, *14*, 31854. [CrossRef] [PubMed]
29. Zhang, C.; Ji, H.; Fu, Z.; Zhang, Y. Analysis of Fracture Characteristics and Energy Evolution of Tectonic Coal after Loading Based on Acoustic Emission. *Measurement* **2025**, *252*, 117388. [CrossRef]
30. Zhang, E.; Dong, X.; Zhu, C.; Zhou, B.; Yu, R.; Gu, L.; Ji, Y. Quantitative Characterization of Failure Evolution in Raw Coal and Briquette Based on Acoustic Emission. *Mech. Adv. Mater. Struct.* **2025**, *32*, 1653–1667. [CrossRef]
31. Zhang, Q.; Pei, J.; Liu, Y.; Li, X.; Nie, B.; Zhang, J.; Liu, H. Study on the Prediction Method for Coal and Rock Mass Fracture Process Based on Time Series Acoustic Emission Statistical Model. *Rock Mech. Rock Eng.* **2025**, *58*, 7631–7647. [CrossRef]
32. Cai, H.; Wang, H.; Huang, T.; Shi, C.; Shi, X.; Chen, Y.; Wei, H. Research on Multi-Source Information Responses and Instability Warning in the Deformation and Failure Process of Coal and Rock. *Sci. Rep.* **2025**, *15*, 42036. [CrossRef] [PubMed]
33. Wang, X.; Wang, J.; Liu, X.; Zhou, X.; Li, N.; Feng, J.; Yang, H. Microcracking Evolution and Clustering Fractal Characteristics in Coal Failure under Multi Step and Cyclic Loading. *Eng. Fract. Mech.* **2024**, *310*, 110511. [CrossRef]
34. Yin, S.; Li, Z.; Wang, E.; Liu, Y.; Niu, Y.; Yang, H. Damage Status and Failure Precursors of Different Coal Impact Types Based on Comprehensive Monitoring of Infrared Radiation and Acoustic Emission. *Appl. Sci.* **2024**, *14*, 8792. [CrossRef]
35. Drozdov, O.V.; Volkov, Y.M. Estimation of the Acoustic Emission Sources Activity Under Mechanical Loading of Materials Based on the Local Dynamic Criterion. *Strength Mater.* **2024**, *56*, 43–52. [CrossRef]
36. Wang, L.; Liu, D.; Wang, S.; Cao, K.; Gao, L. Comparative Study on Stress Acoustic Emission Changes in Damage and Failure of Raw Coal and Briquette. *J. Mine Autom.* **2024**, *50*, 125–134. [CrossRef]
37. Geng, J.; Cao, L.; Zhong, C.; Zhang, S. An Experimental Study on Preparation of Reconstituted Tectonic Coal Samples: Optimization of Preparation Conditions. *Energies* **2021**, *14*, 2846. [CrossRef]
38. Shiotani, T. Parameter Analysis. In *Acoustic Emission Testing: Basics for Research—Applications in Civil Engineering*; Grosse, C., Ohtsu, M., Eds.; Springer: Berlin/Heidelberg, Germany, 2008; pp. 41–51.

https://doi.org/10.3390/app16147057